Ceramics International xxx (xxxx) xxx–xxx

Contents lists available at ScienceDirect

Ceramics International

journal homepage: www.elsevier.com/locate/ceramint

Crystal structure and microwave dielectric properties of $Li_2Mg_{0.6-x}Co_xZn_{0.4}SiO_4$ ceramic for LTCC applications

Maofeng Zhong[a], Hua Su[a,c], Xiaolin Jing[a], Yuanxun Li[a,c], Qihai Lu[b,**], Yulan Jing[a,*]

[a] State Key Laboratory of Electronic Thin Films and Integrated Devices, University of Electronic Science and Technology of China, Chengdu, 610054, China
[b] Key Laboratory of Sensor and Sensing Technology of Gansu Province & Institute of Sensor Technology, Gansu Academy of Sciences, Lanzhou, 730000, China
[c] Jiangxi Xingkang Electronic Technology Co, Ltd, China

ARTICLE INFO

Keywords:
Microwave dielectric properties
LTCC
Solid solution

ABSTRACT

In this work, $Li_2Mg_{0.6-x}Co_xZn_{0.4}SiO_4$ ceramics (x = 0–0.4) added with 3 wt% Li_2O–B_2O_3–Bi_2O_3–SiO_2 (LBBS) glass were synthesised using the solid-state reaction method. The effects of substituting Co^{2+} for Mg^{2+} in $Li_2Mg_{0.6-x}Co_xZn_{0.4}SiO_4$ ceramics on crystal structure, microstructure, densification, crystallisation and microwave dielectric properties were investigated. X-ray diffraction patterns showed that monoclinic Li_2MgSiO_4, monoclinic Li_2ZnSiO_4 and orthorhombic Li_2CoSiO_4 formed finite solid solution in $Li_2Mg_{0.6-x}Co_xZn_{0.4}SiO_4$ ceramics. Clear grain boundaries were observed via scanning electron microscopy. The substitution of Co^{2+} for Mg^{2+} increased grain size, densification, crystallinity degree and dielectric constant; it also reduced the dielectric loss of the ceramics to a certain extent. The absolute values of τ_f were positively related to the crystallinity degree. $Li_2Mg_{0.55}Co_{0.05}Zn_{0.4}SiO_4$ ceramic added with 3 wt% LBBS and sintered at 900 °C exhibited considerable microwave dielectric properties of ε_r = 5.8, $Q \times f$ = 47,518 GHz and τ_f = −74.8 ppm/°C. Therefore, the ceramic is considered a candidate low-temperature co-fired ceramic material for substrate and filter applications.

1. Introduction

Low-temperature co-fired ceramics (LTCC) play important roles in the fields of mobile devices, satellites, telecommunication base stations and transportation systems [1]. These applications have considerable demands for the high frequency, miniaturisation, low energy lost, high integration and multifunctionality of devices. LTCC can meet these requirements by integrating active and passive devices into 3D ceramics co-fired with a low melting point electrode Ag. The sintering temperature of LTCC must be below 950 °C to co-fire with Ag [2]. Thus, different sintering aids have been used to reduce the densification temperature of ceramics for LTCC applications. These sintering aids contain low melting point glasses and inorganic compounds, such as Li_2O–B_2O_3–Bi_2O_3–SiO_2 (LBBS) and lithium fluoride [3–5]. Low relative permittivity (ε_r) is necessary for substrate materials because of the relationship between ε_r and the propagation delay time of the signal: $T_d = L\sqrt{\varepsilon_r}/c$, where L is the distance travelled by the signal, and c is the speed of light [6,7]. $Q \times f$ is the most important property of microwave dielectric ceramics. Low dielectric lost is required to reduce energy lost. The temperature coefficient of resonant frequency (τ_f) is measured to evaluate the temperature stability of dielectric materials [8].

Mg_2SiO_4 and Zn_2SiO_4 exhibit considerable microwave properties: ε_r = 6.8, $Q \times f$ = 240,000 GHz and ε_r = 6.6, $Q \times f$ = 219,000 GHz, respectively. Mg_2SiO_4 and Zn_2SiO_4 are appropriate for substrate applications but unsuitable for LTCC applications because their sintering temperatures are extremely high [9,10]. The substitution of Li^+ for Mg^{2+} and Zn^{2+} can reduce the sintering temperature of Mg_2SiO_4 and Zn_2SiO_4, respectively. The densification temperatures of Li_2MgSiO_4 and Li_2ZnSiO_4 are 1250 °C, which is still extremely high for LTCC applications. Thus, Li_2O–MgO–ZnO–B_2O_3–SiO_2, Li_2O–B_2O_3–SiO_2 and zinc borate glasses have been utilised as sintering aids to reduce densification temperature to approximately 900 °C [11,12]. Considering both Li_2MgSiO_4 and Li_2ZnSiO_4 have low ε_r, the microwave property and microstructure of $Li_2Mg_{1-x}Zn_xSiO_4$ have been studied. The $Li_2Mg_{0.6}Zn_{0.4}SiO_4$ ceramic doped with 3 wt% Li_2O–B_2O_3–SiO_2–CaO–Al_2O_3 and sintered at 900 °C for 3 h presented the following excellent properties: ε_r = 5.89, $Q \times f$ = 44,787 GHz and τ_f = −71 ppm/°C [13]. Some microwave ceramics with lower sintering temperature also were studied recently. For example, Zhang et al. reported the ultra-low temperature sintered microwave dielectric ceramic

* Corresponding author.
** Corresponding author.
E-mail addresses: luqhis20@163.com (Q. Lu), uestcjingyl@163.com (Y. Jing).

https://doi.org/10.1016/j.ceramint.2020.02.081
Received 6 January 2020; Received in revised form 7 February 2020; Accepted 10 February 2020

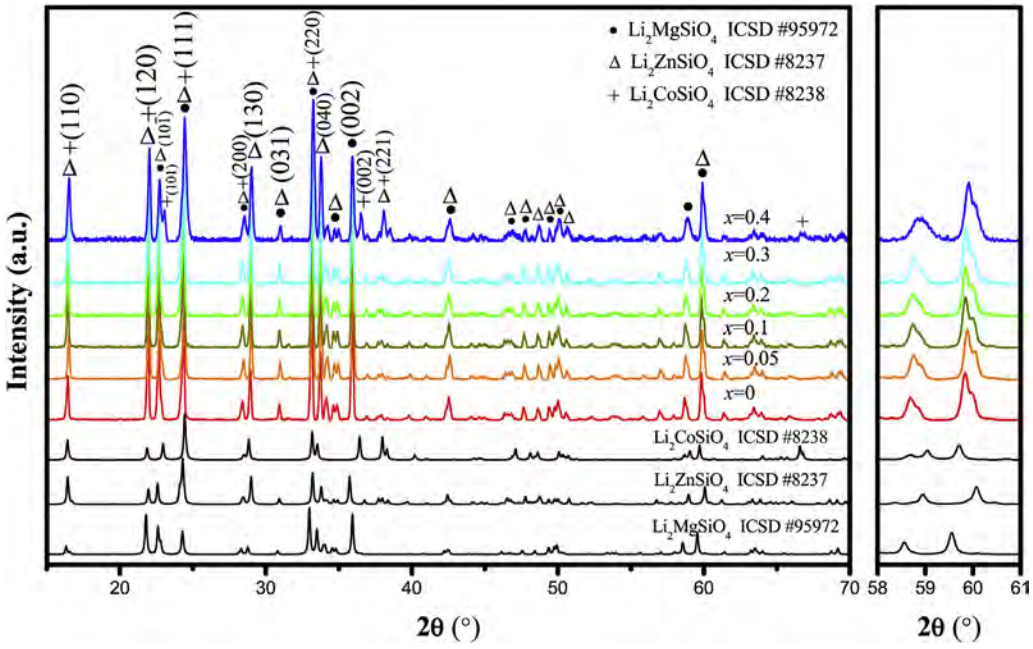

Fig. 1. XRD patterns of the $Li_2Mg_{0.6-x}Co_xZn_{0.4}SiO_4$ ceramics added with 3 wt% LBBS glass and sintered at 900 °C for 4 h.

$Eu_2Zr_3(MoO_4)_9$ with properties of ε_r = 10.75, $Q \times f$ = 74,900 GHz and τ_f = −8.88 ppm/°C, which was sintered at 600 °C for 4 h [14]. Anappropriate amount of Co^{2+} substitution for Zn^{2+} or Mg^{2+} has also been reported to decrease the densification temperature and reduce the dielectric loss of ceramics in previous studies [15–17]. And the effective ionic radii of Mg^{2+}, Zn^{2+} and Co^{2+} are 0.72 Å, 0.74 Å and 0.745 Å, respectively [15]. Because of their close ionic radius, they are more suitable to replace each other. Furthermore, LBBS glass has been reported to be an effective sintering aid for achieving a 900 °C sintered $(Zn_{0.95}Co_{0.05})_2SiO_4$ ceramic [5,18].

In the present study, the microwave dielectric properties of $Li_2Mg_{0.6-x}Co_xZn_{0.4}SiO_4$ (x = 0–0.4) were investigated. Firstly, 3 wt% LBBS was added as sintering aid to decrease sintering temperature to approximately 900 °C. Then, the relationships amongst microstructure, crystal phase, densification, dielectric properties and substitution of Co^{2+} for Mg^{2+} were described in detail.

2. Experimental procedure

$Li_2Mg_{0.6-x}Co_xZn_{0.4}SiO_4$ ceramic (x = 0–0.4) was synthesised using the traditional solid-state reaction method. Analytically pure Li_2CO_3, MgO, CoO, ZnO and SiO_2 were weighed in accordance with their molecular formula and then mixed with deionised water by milling with zirconia balls in a plastic container for 6 h. The derived slurry was dried in an electrically heated drying oven and calcined in alumina crucibles at 900 °C for 3 h. LBBS glass was prepared using a quenching method. The analytical raw materials were weighed at a molar ratio of Li_2CO_3:B_2O_3:Bi_2O_3:SiO_2 = 2:2:1:1. The mixtures were melted at 1100 °C for 4 h in an alumina crucible after milling and drying. The molten LBBS glass was removed from the furnace and immediately quenched in distilled water. The quenched glass was milled into powder for doping. The previous calcined powders were milled again with 3 wt % LBBS glass in plastic containers for 4 h. The wet materials were dried and mixed with polyvinyl alcohol organic binder (10 wt% concentration) and then pressed into cylindrical samples with 12 mm diameter and 6 mm height. The cylindrical samples were sintered at 850 °C–950 °C for 4 h.

The X-ray diffraction (XRD) patterns of the ceramics were measured by an X-ray diffractometer (Rigaku MinFlex 600). The 2θ angle changed from 10° to 120° with a scanning speed of 4°/min. Refinements of the XRD data were conducted using FullProf software with Rietveld's method. The microstructures of the sintered ceramics were observed using a scanning electron microscope (JEOL JSM-6490LV) at an acceleration voltage of 20 kV. The bulk densities of the samples were measured by Archimedes method, and the theoretical densities of the samples were determined from the results of the XRD refinement. The theoretical densities (ρ_{th}) of the crystalline phases were calculated using Formula (1):

$$\rho_{th} = \frac{ZA}{V_C N_A}, \tag{1}$$

where Z, A, V_c and N_A are the number of molecules in a unit cell, the molar molecular weight (g/mol), the volume of the unit cell (cm^3) and Avogadro's constant (mol^{-1}), respectively. For multiphase ceramics, relative density (ρ_r) was calculated using Formula (2):

$$\rho_r = \frac{\sum w_i}{\sum \frac{w_i}{\rho_i}}, \tag{2}$$

where w_i and ρ_i are the weight percentage and theoretical density of phase i, respectively. Microwave dielectric properties were tested by a vector network analyser (Agilent Technologies, N5230A, 300 kHz–20 GHz). The ε_r, $Q \times f$ and resonance frequency of the samples were measured using the Hakki–Coleman dielectric resonator method. The temperature coefficient of resonant frequency was obtained using Formula (3):

$$\tau_f = \frac{f_2 - f_1}{f_1(T_2 - T_1)} \times 10^6, \tag{3}$$

where f_2 and f_1 are the resonant frequencies at temperatures T_2 and T_1 respectively.

3. Results and discussion

The XRD patterns of the samples sintered at 900 °C are shown in Fig. 1, which indicate that the major phases are Li_2MgSiO_4 (ICSD #95972) and Li_2ZnSiO_4 (ICSD #8237), and a minor phase, i.e. Li_2CoSiO_4 (ICSD #8238), is also present. The calculated XRD patterns of the three phases was obtained using Mercury software with K_α = 1.54056 Å. The XRD profiles of the three crystalline phases were

similar due to the similar radii of Mg^{2+}, Zn^{2+} and Co^{2+}. Diffraction peaks (110), (120) and (221) were contributed by phases Li_2ZnSiO_4 and Li_2CoSiO_4. Diffraction peaks (111), (200) and (220) were contributed by all three phases. The exclusive diffraction peaks (101) and (002) of phase Li_2CoSiO_4 were not observed until x increased to 0.4. This phenomenon indicated that substituting Co^{2+} for Mg^{2+} formed a finite solid solution, namely, $Li_2(Mg_{0.6-x}Co_xZn_{0.4})SiO_4$, when $x \leq 0.3$. Two indexes of diffraction peaks that arrived at 58°–61° are not shown in Fig. 1. The details of the profiles can be observed from the amplified XRD pattern. They were contributed by the different diffraction peaks of the various phases. Furthermore, the index of a peak at approximately 42.5° was not shown for the same reason.

All the XRD patterns were refined using FullProf software [19]. Crystal structure, lattice parameters and unit cell volume were obtained by refining the major phase of the XRD data. The structures of Li_2MgSiO_4 with a space group of P 1 21/n 1 (a = 6.3000 Å, b = 10.6920 Å, c = 4.9950 Å, α = 90.00°, β = 90.47° and γ = 90.00°), Li_2ZnSiO_4 with a space group of P 1 21/n 1 (a = 6.2620 Å, b = 10.6020 Å, c = 5.0210 Å, α = 90.00°, β = 90.51° and γ = 90.00°) and Li_2CoSiO_4 with a space group of P b n 21 (a = 6.2530 Å, b = 10.6850 Å, c = 4.9290 Å, α = 90.00°, β = 90.00° and γ = 90.00°) were used as models for refinement. Phases Li_2MgSiO_4 and Li_2ZnSiO_4 were considered for XRD pattern analysis when $x \leq 0.3$. Phases Li_2MgSiO_4, Li_2ZnSiO_4 and Li_2CoSiO_4 were considered for XRD pattern analysis at x = 0.4. The fitted curves of refinement are shown in Fig. 2, and Table 1 summarises the refined results. Agreement factors R_p, R_{wp}, R_{exp} and χ^2 (> 0) were defined as the profile factor, weighted profile factor, expected weighted profile factor and reduced chi-square, respectively. The relation amongst R_{wp}, R_{exp} and χ^2 is $\chi^2 = (R_{wp}/R_{exp})^2$. χ^2 is required to be sufficiently small to ensure the reliability of refinement. The values of χ^2 were smaller than 1.5 in the refinements, indicating that the refinement results were reliable. The lattice parameters and unit cell volumes of the crystals did not change considerably with x. Li_2MgSiO_4, Li_2ZnSiO_4 and Li_2CoSiO_4 crystals coexisted stably in a material system.

The structures of the unit cells of monoclinic Li_2MgSiO_4, monoclinic Li_2ZnSiO_4 and orthorhombic Li_2CoSiO_4 are shown in Fig. 3. The β value of Li_2MgSiO_4 and Li_2ZnSiO_4 were 90.47° and 90.51°, respectively, which were close to 90°. Si^{4+} and O^{2+} are known for forming the tetrahedron [SiO_4], which is the basic structure of silicate. The radii of Li^+, Mg^{2+}, Co^{2+} and Zn^{2+} were similar; thus, they formed a tetrahedron with O^{2+}, i.e. [LiO_4], [MgO_4], [CoO_4] and [ZnO_4], respectively. From the principle of electricity conversion, one O^{2-} connected one tetrahedron [SiO_4], two tetrahedrons [LiO_4] and one tetrahedron [MgO_4]/[ZnO_4]/[CoO_4] for the Li_2MgSiO_4/Li_2ZnSiO_4/Li_2CoSiO_4 structure. The structures of the three crystal phases were similar. Similarity in structure made forming a solid solution possible for these crystal phases.

The microstructures of the $Li_2Mg_{0.6-x}Co_xZn_{0.4}SiO_4$ ceramics added with 3 wt% LBBS and sintered at 900 °C were observed via scanning electron microscopy and shown in Fig. 4. Grain boundaries were evident in all samples, indicating that crystalline grains grew well in these samples. The boundaries of the sample with x = 0.05 were the clearest amongst all samples. Microstructure and morphology are related to microwave dielectric properties [20]. The shape of grains was axiolitic in the sample without Co^{2+} substitution. The shape of grains tended to be claviform with Co^{2+} substitution. Moreover, the substitution of Co^{2+} for Mg^{2+} apparently increased grain size. The average grain sizes of the ceramics and their standard deviations are presented in Fig. 5. Average grain size increased from 2.73 μm to 5.15 μm when Co^{2+} substitution increased from 0 to 0.05 mol. Average grain size did not increase with a continued increase in substitution. Moreover, standard deviation apparently increased from 0.92 to 3.5 μm when substitution increased from 0 to 0.05 mol. These results might be attributed to the following reasons: (1) Co^{2+} increased the grain size of Li_2MgSiO_4 and Li_2ZnSiO_4 to a certain extent, and (2) the grain size of Li_2CoSiO_4 was larger than those of the other two phases.

The bulk and relative densities of the samples sintered at different temperatures are shown in Fig. 6 (a) and (b). Theoretical density was calculated with Formulas (1) and (2) using the unit cell volumes of the refinement results. Weight percentages were calculated in accordance with the molecular formula $Li_2Mg_{0.6-x}Co_xZn_{0.4}SiO_4$. The bulk densities of the samples increased with an increase in Co^{2+} substitution because the weight percentage of Li_2CoSiO_4 increased with an increase in substitution and the theoretical density of Li_2CoSiO_4(3.36 g/cm^3) is higher than that of Li_2MgSiO_4 (2.58 g/cm^3). Moreover, porosity decreased with relative density increased. The relative density of the sample with x = 0.05 and sintered at 900 °C was maximised at 91.3%. This result indicated that Co^{2+} exerted considerable effect on increasing the densification of the ceramics sintered at the same temperature.

The dielectric constant values of the ceramics sintered at different temperatures are shown in Fig. 7 (a). Dielectric constant is related to relative density. High densification corresponds to low porosity. The dielectric constant of porosity is smaller than that of the ceramics. High densification corresponds to high dielectric constant in accordance with the empirical rule of the dielectric constant of composites [21]:

$$\ln \varepsilon = V_1 \ln \varepsilon_1 + V_2 \ln \varepsilon_2, \tag{4}$$

where ε is the dielectric constant of the composite; and ε_1, ε_2, V_1 and V_2 are the dielectric constant of constituent 1, the dielectric constant of constituent 2, the volume fraction of constituent 1 and the volume fraction of constituent 2, respectively. The variation tendencies of dielectric constant and relative density were similar at the same sintering temperature; that is, they increased with the substitution of Co^{2+} for Mg^{2+} and then decreased with further Co^{2+} substitution. This trend demonstrated that an appropriate amount of Co^{2+} substitution for Mg^{2+} increased the densification and dielectric constant of the ceramics. The maximum densification and dielectric constant were 91.3% and 5.8, respectively, when x = 0.05. Moreover, the substitution of Co^{2+} for Mg^{2+} produced the new phase Li_2CoSiO_4. However, the dielectric constants of the composites were not evidently changed by this new phase. This result contributed to the similarity of the dielectric constants of constituents Li_2MgSiO_4, Li_2ZnSiO_4 and Li_2CoSiO_4. The theoretical dielectric constants of Li_2MgSiO_4, Li_2ZnSiO_4 and Li_2CoSiO_4 were 6.15, 7.06 and 6.97, respectively. Their theoretical dielectric constants were calculated using Formulas (5) and (6) [22]:

$$\alpha = \sum_{i=1}^{N} n\alpha_i, \tag{5}$$

$$\varepsilon_r = \frac{V_c + 2b\alpha}{V_c - 2b\alpha}, \tag{6}$$

where α is the polarisability of the composite, and i varies over the total number (N) of ion types in the formula unit. α_i is the polarisability of the ion of type I and n is the number of ion of type i. V_c is the volume of the unit cell, and b is defined as 4π/3.

The $Q \times f$ values of $Li_2Mg_{0.6-x}Co_xZn_{0.4}SiO_4$ sintered at 850 °C–950 °C were presented in Fig. 7 (b). The $Q \times f$ values of the $Li_2Mg_{0.55}Co_{0.05}Zn_{0.4}SiO_4$ ceramic added with 3 wt% LBBS and sintered at 900 °C reached a maximum value of 47,518 GHz in all samples, demonstrating that Co^{2+} exerted considerable impact on reducing dielectric loss. $Q \times f$ values are related to intrinsic loss, such as crystal structure, and nonintrinsic loss, such as densification and crystallisation [23,25]. $Q \times f$ values presented the same variation trend as that of relative density. They both reached a maximum value at x = 0.05. High densification is related to low dielectric loss. Furthermore, the full width at half maximum (FWHM) of the strongest XRD peak (220) is shown in Fig. 8. FWHM is commonly related to ceramic crystallisation. A small FWHM value corresponds to a high crystallinity degree. The FWHM of peak (220) initially decreased and then increased with Co^{2+} substitution for Mg^{2+}, demonstrating that appropriate amount of Co^{2+} could increase crystallinity degree. The minimum FWHM was 0.122°

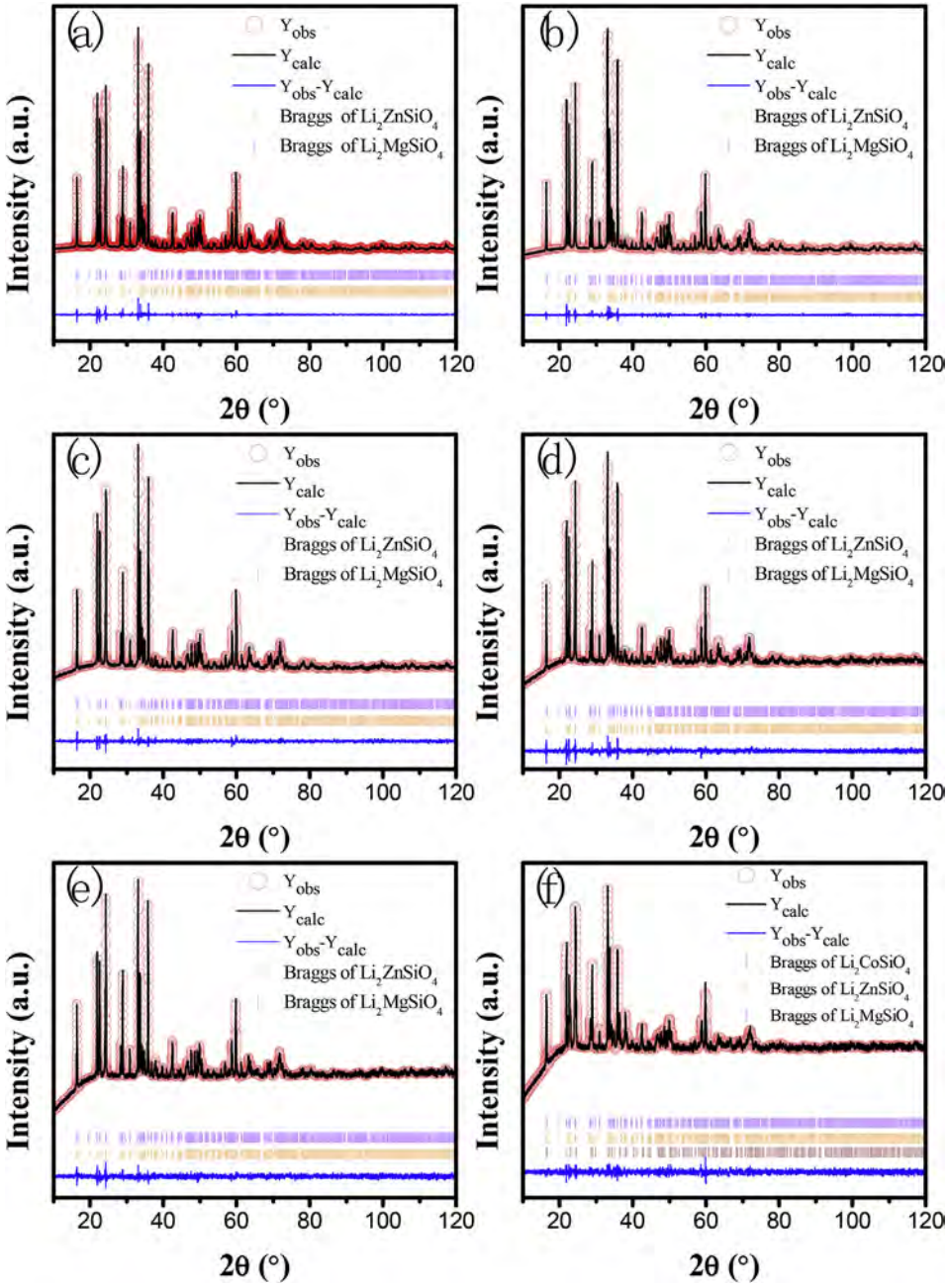

Fig. 2. Rietveld refinements of the $Li_2Mg_{0.6-x}Co_xZn_{0.4}SiO_4$ ceramics added with 3 wt% LBBS glass, (a) $x = 0$, (b) $x = 0.05$, (c) $x = 0.1$, (d) $x = 0.2$, (e) $x = 0.3$, (f) $x = 0.4$.

Table 1
Lattice parameters, unite cell volumes, and agreement factors of the $Li_2Mg_{0.6-x}Co_xZn_{0.4}SiO_4$ ceramics from refinements with Rietveld method.

		$x = 0$	$x = 0.05$	$x = 0.1$	$x = 0.2$	$x = 0.3$	$x = 0.4$
Li_2MgSiO_4	a (Å)	6.28961	6.29412	6.28295	6.29036	6.29327	6.26590
	b (Å)	10.64031	10.65134	10.63763	10.64584	10.65353	10.62538
	c (Å)	5.00599	5.01049	5.00449	5.01131	5.01758	4.99758
	V_c (Å^3)	334.980	335.895	334.466	335.575	336.395	332.724
Li_2ZnSiO_4	a (Å)	6.28398	6.29050	6.27419	6.28773	6.28583	6.23104
	b (Å)	10.63728	10.65221	10.63105	10.64738	10.65107	10.60429
	c (Å)	5.00255	5.00772	5.00032	5.01155	5.01358	5.00046
	V_c (Å^3)	334.381	335.544	333.515	335.500	335.650	330.393
Li_2CoSiO_4	V_c (Å^3)						326.198
	R_p (%)	7.22	8.27	14.8	17.3	22.6	22.1
	R_{wp} (%)	7.98	7.76	10.6	12.5	13.3	15.3
	R_{exp} (%)	7.27	8.60	11.4	13.35	16.65	18.33
	χ^2	1.20	0.8130	0.859	0.873	0.636	0.694

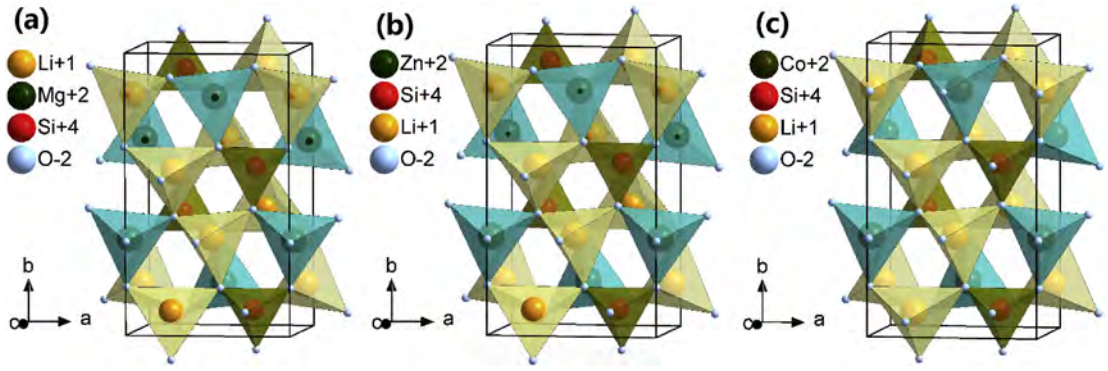

Fig. 3. Crystal structures based on the data of ICSD, (a) Li_2MgSiO_4, (b) Li_2ZnSiO_4, (c) Li_2CoSiO_4.

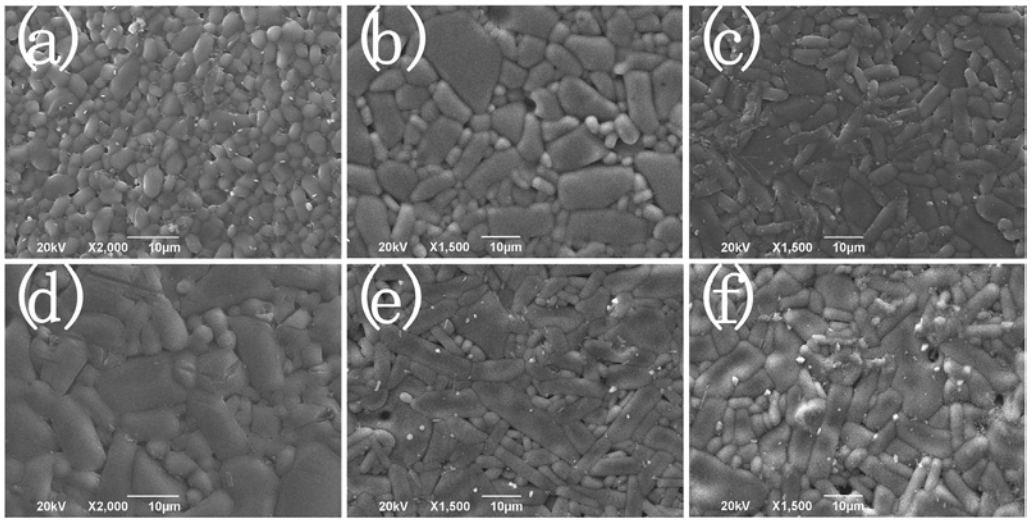

Fig. 4. SEM photos of the $Li_2Mg_{0.6-x}Co_xZn_{0.4}SiO_4$ ceramics added with 3 wt% LBBS glass and sintered at 900 °C, (a) $x = 0$, (b) $x = 0.05$, (c) $x = 0.1$, (d) $x = 0.2$, (e) $x = 0.3$, (f) $x = 0.4$.

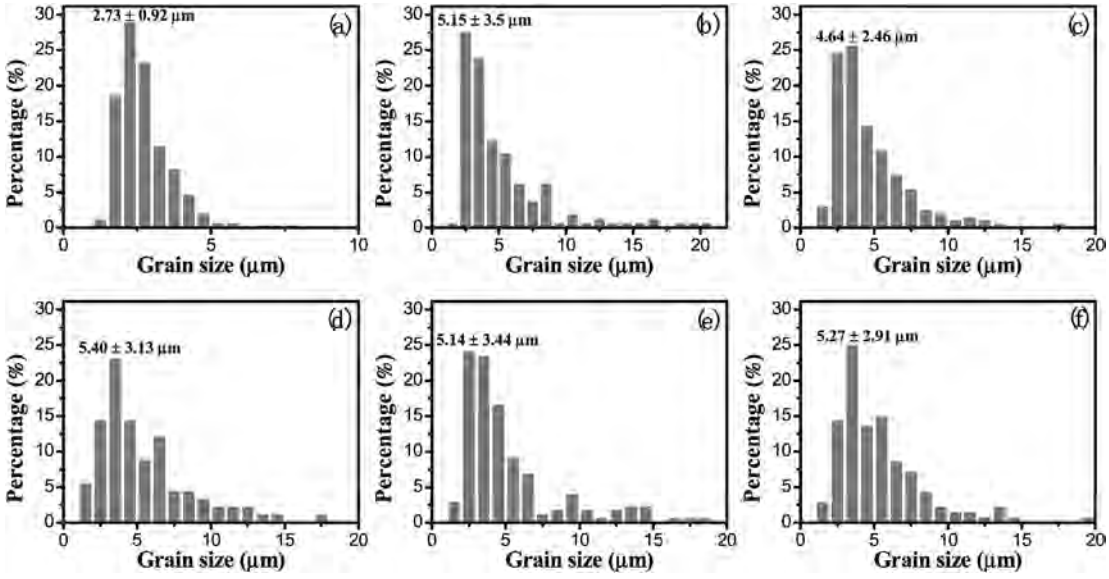

Fig. 5. Statistics of grain sizes of the $Li_2Mg_{0.6-x}Co_xZn_{0.4}SiO_4$ ceramics added with 3 wt% LBBS and sintered at 900 °C, (a) $x = 0$, (b) $x = 0.05$, (c) $x = 0.1$, (d) $x = 0.2$, (e) $x = 0.3$, (f) $x = 0.4$.

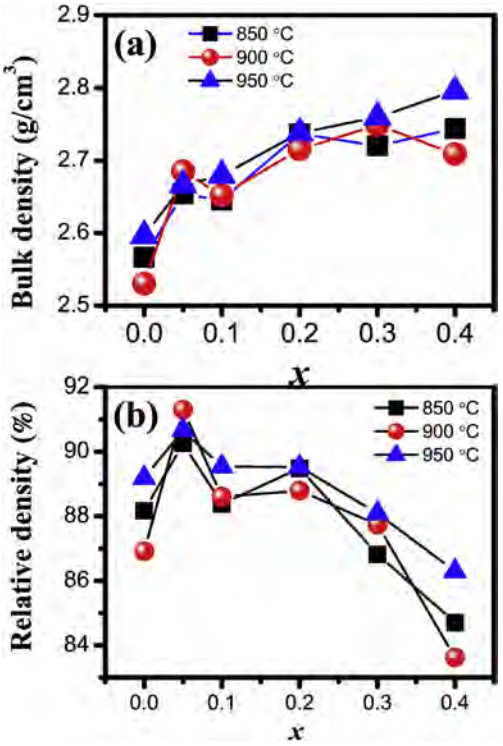

Fig. 6. Density and relative density of the $Li_2Mg_{0.6-x}Co_xZn_{0.4}SiO_4$ ceramics added with 3 wt% LBBS and sintered at 850 °C–950 °C.

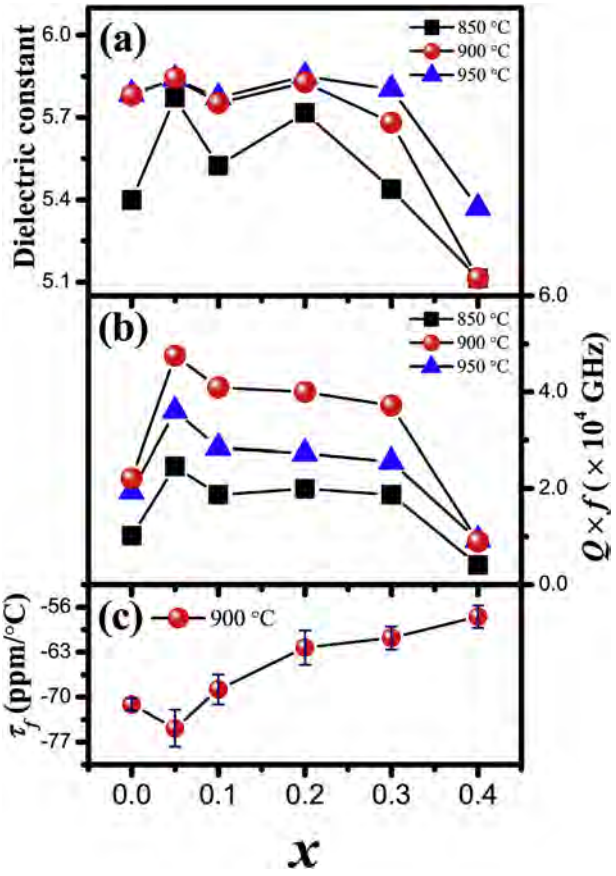

Fig. 7. Dielectric properties of the $Li_2Mg_{0.6-x}Co_xZn_{0.4}SiO_4$ ceramics added with 3 wt% LBBS and sintered at 850 °C–950 °C, (a) dielectric constant, (b) $Q \times f$, (c) τ_f.

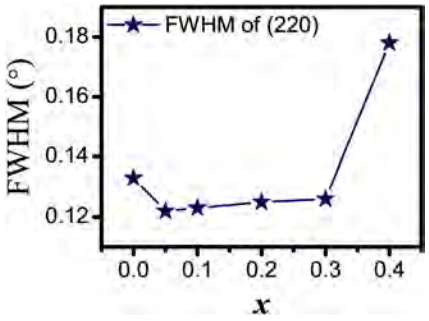

Fig. 8. FWHM of XRD peak (220) of the $Li_2Mg_{0.6-x}Co_xZn_{0.4}SiO_4$ ceramics added with 3 wt% LBBS and sintered at 900 °C.

when $x = 0.05$. The $Q \times f$ values were related to the FWHM of the XRD peak (220) for the $Li_2Mg_{0.6-x}Co_xZn_{0.4}SiO_4$ ceramics.

The τ_f of the samples sintered at 900 °C is shown in Fig. 7 (c), and it varied from −57.5 ppm/°C to −74.8 ppm/°C with x. τ_f is related to the structure and temperature coefficient of the dielectric constant of compounds [24,25]. It initially decreased and then increased with Co^{2+} substitution for Mg^{2+} sintered at 900 °C. The same variation was observed in the FWHM of the XRD peak (220) in Fig. 8. Given that FWHM is related to crystallinity degree, the absolute values of τ_f are positively related to crystallinity degree. Moreover, the phase Li_2CoSiO_4 produced by the substitution of Co^{2+} for Mg^{2+} might have exerted an impact on τ_f. On the whole, the τ_f values of the $Li_2Mg_{0.6-x}Co_xZn_{0.4}SiO_4$ ceramics were more negative. Other constituents with large positive τ_f values, such as $CaTiO_3$ and TiO_2, are commonly used to adjust τ_f values to around zero [26,27]. Furthermore, some types of ion substitution could also effectively adjust τ_f values. An appropriate amount of Cu^{2+} substitution for Mg^{2+} adjusted τ_f value of the $Mg_{2-x}Cu_xSiO_4$ ceramic by modifying the distortion of MgO6 octahedron [25]. Similarly, an appropriate amount of Ti^{4+} substitution for Zr^{4+} adjusted the τ_f value of $La_2(Zr_{1-x}Ti_x)_3(MoO_4)_9$ ceramic, which indicated that the τ_f value was also closely related to the coefficient of thermal expansion and bond valence [28]. In the next study, we will analyze the influence of octahedral distortion ion substitution on the temperature coefficient and dielectric properties of the ceramics.

4. Conclusions

The effects of substituting Co^{2+} for Mg^{2+} on crystal phase, microstructure, densification and microwave dielectric properties were investigated in the present work. Phases Li_2MgSiO_4, Li_2ZnSiO_4 and Li_2CoSiO_4 formed a solid solution in the composite ceramics. Co^{2+} influenced the grain size, densification, crystallinity degree and microwave dielectric properties of ceramics. Excellent microwave dielectric properties of $\varepsilon_r = 5.8$, $Q \times f = 47{,}518$ GHz and $\tau_f = -74.8$ ppm/°C were obtained at $x = 0.05$ and sintered at 900 °C. Thus, $Li_2Mg_{0.55}Co_{0.05}Zn_{0.4}SiO_4$ ceramic added with 3 wt% LBBS can be an alternative LTCC material for substrate and filter applications.

Declaration of competing interest

The authors declare that they have no known competing financial interests or personal relationships that could have appeared to influence the work reported in this paper.

Acknowledgements

This work was supported by the National Natural Science Foundation of China under Grant Nos. 61771104, U1809215 and 61871069.

References

[1] X. Song, W. Lu, X. Wang, X. Wang, G. Fan, Sintering behaviour and microwave dielectric properties of $BaAl_{2-2x}(ZnSi)_xSi_2O_8$ ceramics, J. Eur. Ceram. Soc. 38 (2018) 1529–1534, https://doi.org/10.1016/j.jeurceramsoc.2017.10.053.

[2] M.T. Sebastian, R. Ubic, H. Jantunen, Low-loss dielectric ceramic materials and their properties, Int. Mater. Rev. 60 (2015) 392–412, https://doi.org/10.1179/1743280415_Y.0000000007.

[3] M.T. Sebastian, H. Jantunen, Low loss dielectric materials for LTCC applications: a review, Int. Mater. Rev. 53 (2008) 57–91, https://doi.org/10.1179/174328008X277524.

[4] X. Du, H. Su, H. Zhang, Y. Jing, Z. Zhou, G. Gan, Effects of Li-ion substitution on the microwave dielectric properties of low- temperature sintered ceramics with nominal composition $Li_{2x}Mg_{2-x}SiO4$, Ceram. Int. 44 (2018) 2300–2303, https://doi.org/10.1016/j.ceramint.2017.10.193.

[5] Y. Lai, H. Su, G. Wang, X. Tang, X. Huang, X. Liang, H. Zhang, Y. Li, K. Huang, X.R. Wang, Low-temperature sintering of microwave ceramics with high *Qf* values through LiF addition, J. Am. Ceram. Soc. 102 (2019) 1893–1903, https://doi.org/10.1111/jace.16086.

[6] H. Yu, J. Liu, M. Zeng, L. He, Structure and dielectric properties of zinc borate glass – ceramics modified by magnesium, J. Mater. Sci. Mater. Electron. 27 (2016) 7109–7114, https://doi.org/10.1007/s10854-016-4673-4.

[7] G.T. Division, H. Junction, Review of multilayer ceramics for microelectronic packaging, J. Phys. Chem. Solid. 45 (1984) 1051–1068, https://doi.org/10.1016/0022-3697(84)90048-9.

[8] X. Song, K. Du, J. Li, X. Lan, W. Lu, X. Wang, Low-fired fluoride microwave dielectric ceramics with low dielectric loss, Ceram. Int. 45 (2019) 279–286, https://doi.org/10.1016/j.ceramint.2018.09.164.

[9] T. Tsunooka, M. Androu, Y. Higashida, H. Sugiura, H. Ohsato, Effects of TiO_2 on sinterability and dielectric properties of high - *Q* forsterite ceramics, J. Eur. Ceram. Soc. 23 (2003) 2573–2578, https://doi.org/10.1016/S0955-2219(03)00177-8.

[10] Y. Guo, H. Ohsato, K. Kakimoto, Characterization and dielectric behavior of willemite and TiO_2 - doped willemite ceramics at millimeter-wave frequency, J. Eur. Ceram. Soc. 26 (2006) 1827–1830, https://doi.org/10.1016/j.jeurceramsoc.2005.09.008.

[11] S. George, P.S. Anjana, V.N. Deepu, P. Mohanan, M.T. Sebastian, Low-temperature sintering and microwave dielectric properties of Li_2MgSiO_4 Ceramics, J. Am. Ceram. Soc. 92 (2009) 1244–1249, https://doi.org/10.1111/j.1551-2916.2009.02998.x.

[12] G. Dou, D. Zhou, S. Gong, M. Guo, Low temperature sintering and microwave dielectric properties of Li_2ZnSiO_4 ceramics with ZB glass, J. Mater. Sci. Mater. Electron. 24 (2013) 1601–1607, https://doi.org/10.1007/s10854-012-0982-4.

[13] X. Jing, X. Tang, W. Tang, Y. Jing, Y. Li, H. Su, Effects of Zn^{2+} substitution on the sintering behaviour and dielectric properties of $Li_2Mg_{1-x}ZnxSiO_4$ ceramics, Appl. Phys. A 125 (2019) 1–6, https://doi.org/10.1007/s00339-019-2712-8.

[14] Y.H. Zhang, J.J. Sun, N. Dai, Z.C. Wu, H.T. Wu, C.H. Yang, Crystal structure, infrared spectra and microwave dielectric properties of novel extra low-temperature fired $Eu_2Zr_3(MoO_4)_9$ ceramics, J. Eur. Ceram. Soc. 39 (2019) 1127–1131, https://doi.org/10.1016/j.jeurceramsoc.2018.12.042.

[15] R.D. Shannon, Revised effective ionic radii and systematic studies of interatomic distances in halides and chalcogenides, Acta Crystallogr. 32 (1976) 751–767, https://doi.org/10.1515/ehs-2015-0001.

[16] H.W. Chen, H. Su, H.W. Zhang, T.C. Zhou, B.W. Zhang, J.F. Zhang, X.L. Tang, Low-temperature sintering and microwave dielectric properties of $(Zn_{1-x}Co_x)_2SiO_4$ ceramics, Ceram. Int. 40 (2014) 14655–14659, https://doi.org/10.1016/j.ceramint.2014.06.053.

[17] A. Ullah, H. Liu, Z. Pengcheng, H. Hao, J. Iqbal, M. Cao, Z. Yao, Influence of Co substitution on the phase, microstructure, and microwave dielectric properties of $MgSiO_3$ ceramics, J. Mater. Sci. Mater. Electron. 30 (2019) 6469–6474, https://doi.org/10.1007/s10854-019-00951-8.

[18] Z. Zhou, H. Su, X. Tang, H. Zhang, F. Xu, S. Zhang, Y. Jing, Microwave dielectric properties of LBBS glass added $(Zn_{0.95}Co_{0.05})_2SiO_4$ for LTCC technology, Ceram. Int. 42 (2016) 11161–11164, https://doi.org/10.1016/j.ceramint.2016.04.022.

[19] Y. Lai, C. Hong, L. Jin, X. Tang, H. Zhang, X. Huang, J. Li, H. Su, Temperature stability and high-Qf of low temperature firing Mg_2SiO_4–Li_2TiO_3 microwave dielectric ceramics, Ceram. Int. 43 (2017) 16167–16173, https://doi.org/10.1016/j.ceramint.2017.08.192.

[20] Y. Lai, X. Tang, H. Zhang, X. Liang, X. Huang, Y. Li, Correlation between structure and microwave dielectric properties of low- temperature- fi red Mg_2SiO_4 ceramics, Mater. Res. Bull. 99 (2018) 496–502, https://doi.org/10.1016/j.materresbull.2017.11.036.

[21] Y. Imanaka, Multilayered Low Temperature Cofired Ceramics (LTCC) Technology, Springer, Boston, MA, 2005, p. 112, https://doi.org/10.1007/b101196.

[22] R.D. Shannon, F.L.D. Shannon, Dielectric polarizabilities of ions in oxides and fluorides Dielectric polarizabilities of ions in oxides and fluorides, J. Appl. Phys. 73 (1993) 348–366, https://doi.org/10.1063/1.353856.

[23] B. Tang, Q. Xiang, Z. Fang, X. Zhang, Z. Xiong, H. Li, In fluence of Cr^{3+} substitution for Mg^{2+} on the crystal structure and microwave dielectric properties of $CaMg_{1-x}Cr_{2x/3}Si_2O_6$ ceramics, Ceram. Int. 45 (2019) 11484–11490, https://doi.org/10.1016/j.ceramint.2019.03.016.

[24] K. Du, X. Song, J. Li, J. Wu, W. Lu, X. Wang, Optimised phase compositions and improved microwave dielectric properties based on calcium tin silicates, J. Eur. Ceram. Soc. 39 (2019) 340–345, https://doi.org/10.1016/j.jeurceramsoc.2018.10.005.

[25] Y. Lai, X. Tang, X. Huang, H. Zhang, X. Liang, J. Li, H. Su, Phase composition, crystal structure and microwave dielectric properties of $Mg_{2-x}Cu_xSiO_4$ ceramics, J. Eur. Ceram. Soc. 38 (2018) 1508–1516, https://doi.org/10.1016/j.jeurceramsoc.2017.10.035.

[26] G. Dou, M. Guo, Y. Li, Effects of $CaTiO_3$ on microwave dielectric properties of Li_2ZnSiO_4 ceramics for LTCC, J. Mater. Sci. 27 (2016) 359–364, https://doi.org/10.1007/s10854-015-3762-0.

[27] J. Sugihara, K. Kakimoto, I. Kagomiya, H. Ohsato, Microwave dielectric properties of porous Mg_2SiO_4 filling with TiO_2 prepared by a liquid phase deposition process, J. Eur. Ceram. 27 (2007) 3105–3108, https://doi.org/10.1016/j.jeurceramsoc.2006.1S1.032.

[28] Y. Zhang, H. Wu, Crystal structure and microwave dielectric properties of $La_2(Zr_{1-x}Ti_x)_3(MoO_4)_9$ ($0 \leq x \leq 0.1$) ceramics, J. Am. Ceram. Soc. 102 (2019) 4092–4102, https://doi.org/10.1111/jace.16268.